Journal of Mines, Metals and Fuels, *72(4): 391-400; 2024. DOI: 10.18311/jmmf/2024/44052*

INFORMATICS JOURNALS

Print ISSN : 0022-2755

Journal of Mines, Metals and Fuels

Contents available at: *www.informaticsjournals.com/index.php/jmmf*

Sliding Wear Characteristics of Zn-15Sn Alloy with Nano B_4C Reinforced Composites

Santosh V. Janamatti[1], Raju Jadar[1], S. B. Angadi[2], Nagaraj Namdev[3], Subbaraya Mohan Kumar[4], Madeva Nagaral[5]* and A. N. Prashanth[5]

[1]*Mechanical Engineering Department, Ballari Institute of Technology and Management, Ballari - 583102, Karnataka, India*

[2]*Department of Mechanical Engineering, KLE Technological University, Dr. M. S. Sheshgiri Campus, Belagavi - 590008, Karnataka, India*

[3]*Department of Mechanical Engineering, APS Polytechnic, Bengaluru - 560082, Karnataka, India*

[4]*Department of Mechanical Engineering, Jyothy Institute of Technology, Bengaluru - 560082, Karnataka, India.*

[5]*Aircraft Research and Design Centre, HAL, Bengaluru - 560037, Karnataka, India; madev.nagaral@gmail.com*

Abstract

In the current investigation, high pin-on-disc wear testing equipment was used to examine the impact of modest additions of nano B_4C on the wear behaviour of a Zn alloy (85Zn-15Sn). Zn-Sn alloy behaviour at a constant SD of 2000m under pressures (10N, 20N, 30N, and 40N) and sliding speeds (1.4, 1.8, 2.3 and 2.8 m/s) was investigated. Microanalysis with SEM/EDX was used to characterise the matrix and worn surfaces. According to the results, the wear rate of Zn alloy rises with rising pressures, sliding speeds and distances in all situations examined and lowers with an additional level of 8 weight per cent B_4C to the Zn alloy when tested. This is brought on by the partial refinement of Zn dendrites, as well as the precipitation hardening of solid solutions. The worn surface investigation suggests that the creation of a thick oxide layer during sliding enhances tribological features.

Keywords: *B_4C Particulates, Sliding Speed and Load, Stirs Casting, Wear Mechanism, Zn85-Sn15*

1.0 Introduction

Advanced manufacturing has led to an increase in demand for tribological mechanisms under challenging wear conditions, such as high sliding speeds, and high applied loads and in a variety of industrial applications, including automotive, marine engineering, power generation and material processing[1,2]. Aluminium-magnesium alloys have tremendous scope among the materials of tribological significance for both practical and theoretical reasons[3,4]. Among the several foundry alloys, they are the most significant, accounting for 70% of the castings of copper[5-8]. It has been proved that copper and aluminium alloys have desirable mechanical and physical characteristics for use in applications involving long sliding distances[1]. A range of hypoeutectic alloys includes ZA12 (88Zn-11Al-1Cu-0.02Mg). It is observed that strengthening aluminium alloys with minor additions of Cu, Mg, Zn and the presence of Zn results in excellent casting characteristics[9-11]. By strengthening a metal and causing precipitation (AGE) hardening, alloying elements result in a high strength-to-weight ratio[12]. According to

Author for correspondence

past studies, nano B_4C significantly improves the strength and hardness under both as-cast and heat-treated conditions. Madeva Nagaral[13] investigated how adding nano B_4C affected the wear properties of Al2618 base alloys and found that 6-weight per cent B_4C solidified in graphite moulds provided the optimum mechanical properties. Additionally, they claimed that increasing B_4C reinforcement had led to a partial refinement of dendrites. When the aggregation is reduced, the casting microstructure becomes finer. The tensile characteristics of cast parts will therefore be improved as a result. The outcomes additionally demonstrate that the UTS rises with nano B_4C content up to 6wt%. The precipitation of the boron-bearing phase in interdendritic gaps brought on by rising boron carbide causes an increase in UTS. Recently, Manjunath TH *et al.*[14] concluded that small additions of boron carbide, such as 2% to A18081 alloy course refine the nanoparticles of B_4C improving the wear properties of Al1808 alloy and 6% B_4C addition to Al-1808 alloy shows improvement in proof stress, UTS and % elongation matched to smaller additions of B_4C and the as-cast conditions. According to Radhakrishna and Ramesh[15], the mixing of B_4C, Cu and Mg enhances the basic mechanical properties through precipitation hardening, as noted by Abbas *et al.*[16] and B T Ramesh *et al*[12] . It can boost the transition load and wear resistance even further. Veereshkumar G. B.[17] examined the impact of B_4C introduction on Al3003-Sic alloys and concluded that the introduction of B_4C enhances the alloy's tribological mechanism of a selected ally. Most industrial applications requiring wear and friction pistons[18], cylinder heads and engine blocks for automobiles[19] are three instances where temperatures considerably beyond 200 to 300 °C can be anticipated[20]. In the current study, an effort has been made to investigate the impact of B_4C addition wear behaviour of Zn-Sn alloy under various parameters.

2.0 Details of Experimental

2.1 Fabrication of Wear Samples

A ceramic crucible held in a resistance furnace[21] was used to melt the commercial Zn-Sn alloy (1000g). A commercial degasser made of potassium titanium fluoride (K2TiT6) was used to degas the molten metal at a temperature of 720°C to eliminate hydrogen. The Zn-Sn-B_4C alloy chips were properly sued and then added to melt after degassing. After adding the Zn alloy, the melt was stirred with an iron rod coated in Zirconia for five minutes at a speed of 300rpm. Thereafter, no additional stirring was done. Melts were poured into split-type graphite moulds[22] (25mm diameter and 120mm height) for the preparation of wear that was used to prepare specimens for microstructural studies. The melt without the composite alloy is indicated by the number 0 minutes. As per ASTM G99 standards[23-25], the wear test pin was 8mm in diameter and 30mm in length[14]. Using an atomic absorption spectrometer, the chemical composition of Zn-Sn alloy and Zn-Sn- B_4C composite alloy was determined and is displayed in Table 1.

Table 1. Zn-Sn alloy and its nano B4C composites with a standard deviation

Material Composition	Hardness (BHN)
Zn-Sn Alloy	82.03 ± 1.50
Zn-Sn – 2 wt. % B4C	88.53 ± 1.43
Zn-Sn – 4 wt. % B4C	100.20 ± 1.15
Zn-Sn – 6 wt. % B4C	115.02 ± 1.16

± - SD (Standard Deviation)

2.2 Details of Wear Test

The present studies were performed using a pin-on-disc[22] wear testing equipment to address the wear behaviour of Zn-Sn-B_4C alloys with varying compositions. The test pin was used opposite to the disc using a pulley system and a dead weight. En-31 steel, with a hardness grade of HRC 61 was used to make the disc[1]. It measured 165mm in diameter and 8mm in thickness. The surface roughness of the disc ranges from 0.47 to 0.87m. The tests were performed under dry sliding circumstances[26].The highest loading capacity of the system was 200 N. Throughout the testing, the track diameter was fixed at 90mm and consistently used[27]. The sliding experiments were performed under a range of conditions, including varying pressure, varying sliding speeds and varying sliding speeds. Table 2 displays test information in detail. SEM, EDX and X-ray microanalysis were used to characterise papered composite samples[28].

3.0 Results and Discussions

3.1 Microstructural Analysis

Using SEM metallographic measurements were produced. The elements were measured using EDX microanalysis[29]. The typical method of polishing metallographic specimens was used, but the final polishing was done by hand with 3m diamond pastes. The SEM micrographs of Zn alloy with various weight percentage additions of B_4C alloy are shown in Figure 1a–e. According to the microstructural

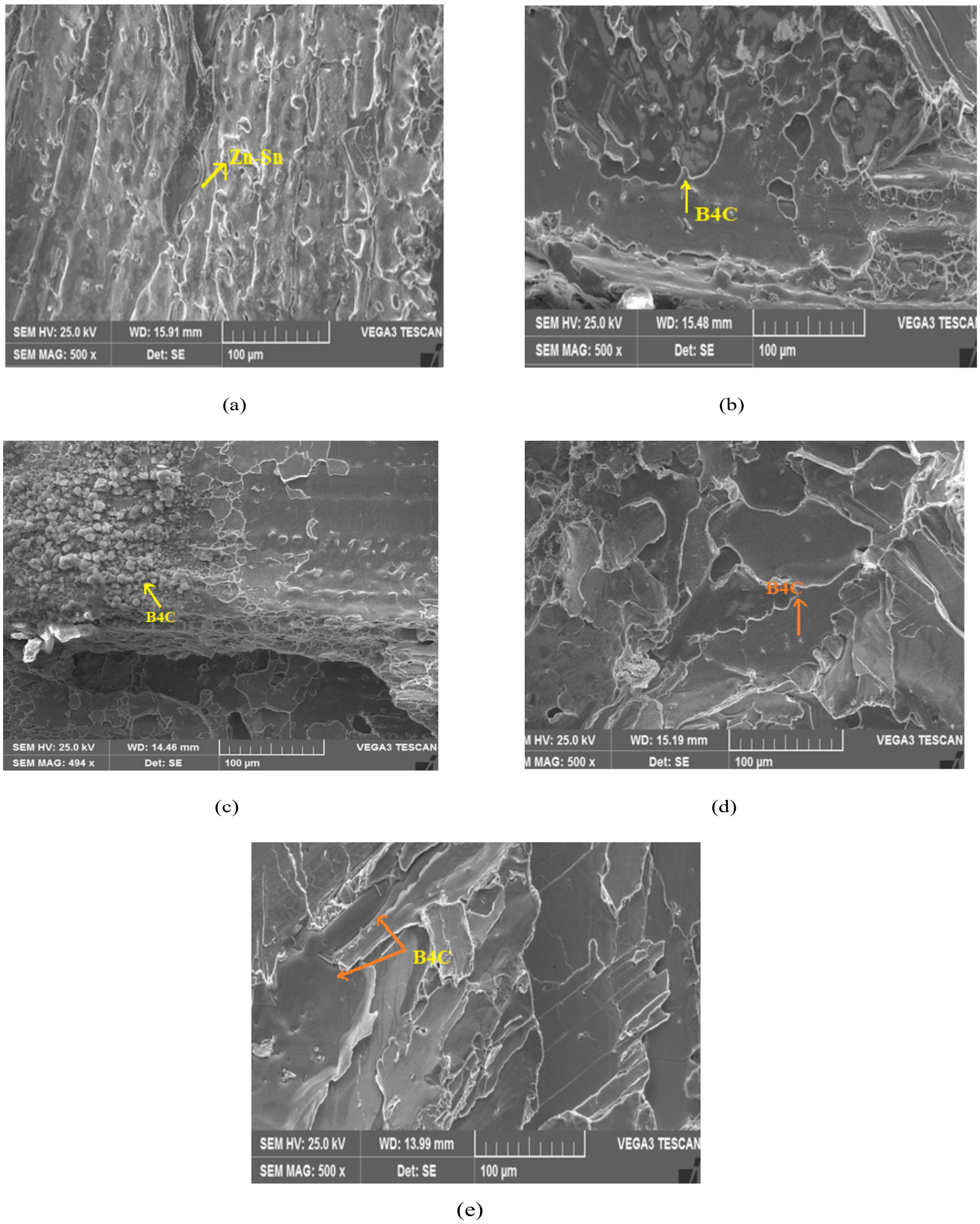

Figure 1. The SEM image of Zn-Sn **(a)** as-cast alloy, **(b)** with 2% B_4C **(c)** with 4% B_4C, **(d)** with 6% B_4C and **(e)** with 8% B_4C.

analysis, Zn-Sn alloy exhibits an unaltered needle/plate-like eutectic Sn and coarse columnar -Zn dendritic structure without B_4C (Figure. 1(a)). Although there is a structural change from coarse columnar dendritic structure to coarse equiaxed structure and eutectic boron carbide stays larger addition of 8% B_4C exhibits fine and well dispersion eutectic boron phase[30] (Figure. 1(e)). This is brought on by growing nano-boron carbide addition's partial refinement of dendrites[23,31–33]. This might be because the Zn-15% Sn alloy also contains intermetallic particles B_4C, which promote heterogeneous nucleation during solidification.

3.2 Wear Studies

3.2.1 Effects of Pressure

The impact of different pressures (10N, 20N, 30N, and 40N) on the removal rate and frictional force of the Zn-Sn alloy matrix and the addition of 8% B_4C is depicted in Figures. 2(a) and (b). It is evident from Figure 2(a), that the rate of wear of Zn-Sn alloy is higher with higher pressure fabricated compositions examined. This higher wear rate with higher pressure is consistent with Archard's wear law. When the pressure is raised, the wear rate rises dramatically from 0.33 to 2.24mm^3/m in the case of cast alloy and from 0.55 to 1mm^3/m in the case of 8wt% B_4C reinforcement. The pressure of 40N indicates extreme wear in the case of Zn-Sn alloy. When the pin slides, the majority of the metal is moved from it to the steel counter face in areas with extreme wear, but in areas with less wear, the pin oxidises and slides without any bulk metal move[1]. The matrix becomes soft at greater loads, which increases the surface contact and temperature of the pin and increases the wear rate. More specifically, the rate of material removed ranged from 0.32 to 2.24mm^3/m. As seen in Figure 2a, the Zn-Sn alloy exhibits an extreme mode of wear at 2.24mm^3/m. Zn-Sn alloy with an addition of 8 weight per cent B_4C exhibits a lower rate of wear than cast alloy under the same test conditions. This is a result of increased strength and hardness of the matrix[23,31–37]. In all the examples investigated, frictional force increased with the rising normal pressures. However, it decreased with the addition of 8 weight per cent of B_4C to the Zn-Sn alloy, as shown in Figure 2(b). This decrease in frictional force was caused by the softness of the Zn-Sn alloy relative to the reinforced alloy. Increased normal pressure makes the Zn-Sn alloy sufficiently flexible, allowing for close contact between the pin and the disc, softening the Zn alloy matrix, which reduces frictional force[12]. It can be seen from Figure 2(b) that regardless of the pressures used, the frictional force for the alloy with the addition of boron carbide is larger than that of the alloy as cast. At 8wt% B_4C to Zn-alloy, the mechanical properties have improved[15,31,38,39].

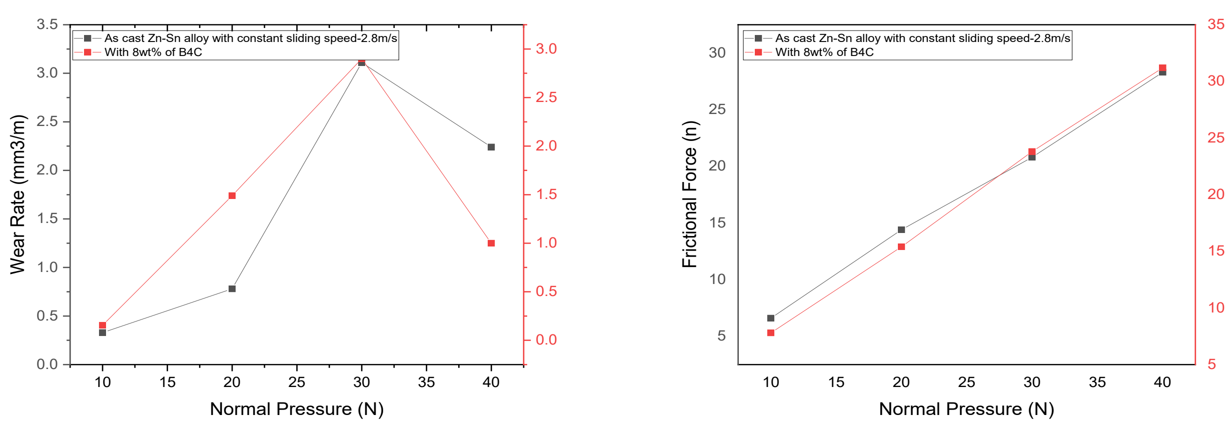

(a) (b)

Figure 2. The impact of varying normal pressures on the **(a)** wear rate of Zn-Sn alloy with base alloy and addition of 8wt% B4C; **(b)** FF of Zn-Sn alloy with addition 8wt% B4C.

3.2.2 Effect of Sliding Speeds

In Figure 3(a), the wear rate is depicted as a function of the sliding speed (14m/s, 1.8m/s, 2.3m/s and 2.8m/s) and the constant normal pressure (40N) at a constant distance (2000m) from the sliding surface. Both treated and untreated alloys initially exhibit increased wear conditions, which are sustained up to 1.4m/s after which the slope of the wear curve changes, suggesting the beginning of decreased wear in the case of Zn-Sn alloy. When the alloy is sliding at 2.8m/s, wear starts to decrease, but under the same test conditions, a Zn-Sn alloy with an addition of 8 weight per cent of B_4C is still only experiencing light wear. The Zn alloy's enhanced matrix strength and microstructural modifications are responsible for this[23,30–37,40]. Additionally, the development of a layer that is mechanically mixed and results in a slower rate of wear could be the cause. By looking at the graph, it can be seen that both with and without B_4C reinforcement, the wear rate condition is quite moderate at 2.8m/s. Sliding causes a decrease in wear rate, as evidenced by these studies.

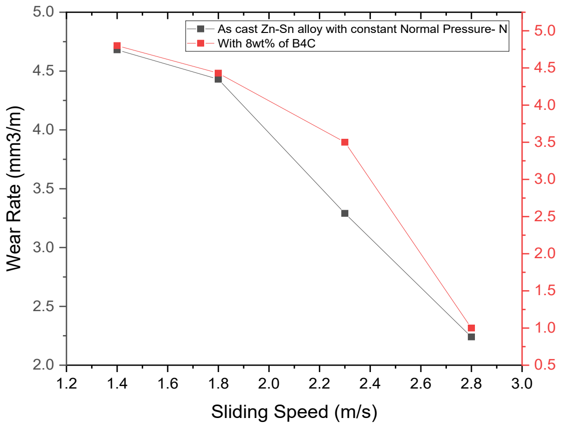

(a)

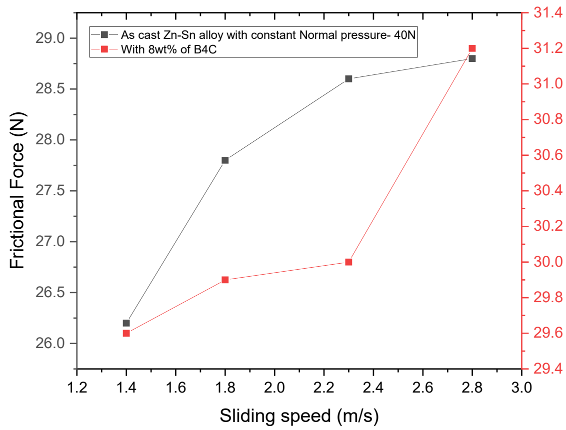

(b)

Figure 3. The impact of varying sliding speeds on the **(a)** wear rate of Zn-Sn alloy with the addition of 8wt% of B_4C; **(b)** FF of Zn-Sn alloy with the addition of 8wt% of B_4C.

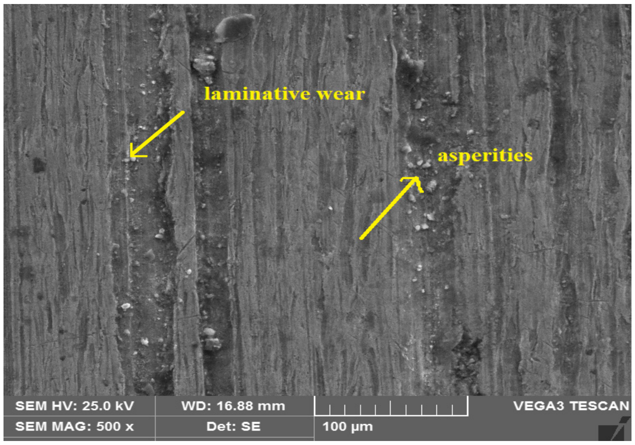

(a)

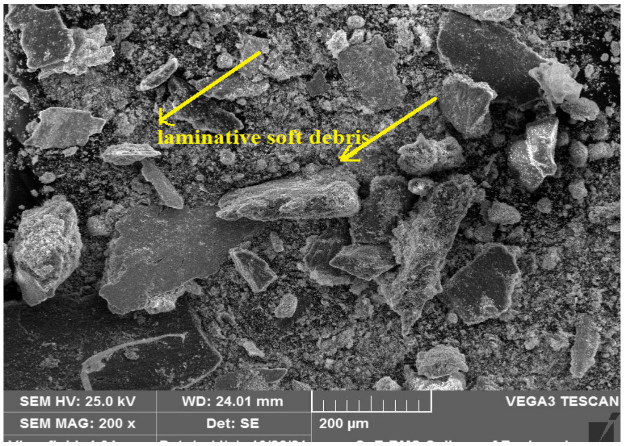

(b)

Figure 4. **(a)**. SEM micrograph of Zn alloy specimen, speed-1.4 m/s, load 10N. **(b)** Wear debris micrograph of Zn alloy specimen, speed-1.4 m/s, load 10N with 2000m sliding distance.

Comparably, Figure 3(b) illustrates how the frictional force of a Zn-Sn alloy changes depending on the sliding speed. For a cast alloy, the amount of friction increases with the rate of sliding. Under comparable test conditions, a Zn-Sn alloy with an addition of 8 weight per cent of B_4C exhibits higher frictional force as sliding speeds increase, but this increase is more than that of the cast alloy. Due to increasing formation oxidation between both surfaces during sliding, the frictional force somewhat shows a high sliding speed of 2.8 m/s.

3.3.3 Worn-Out Surface Studies

The worn surface of a Zn-Sn alloy was examined using SEM and EDS. The wear surface of a Zn-Sn alloy at 10N and 1.4m/s is shown in Figure 4(a). It is evident from Figure 4a that the worn surface has both continuous and irregular grooves, which have been caused by the abrasion of entrapped particles[41]. This shows that at mild applied pressure, mild abrasive wear is more common. It is evident from Figure 4(b) that shows soft laminative wear debris at a pressure of 40N and a speed of 2.8m/s.

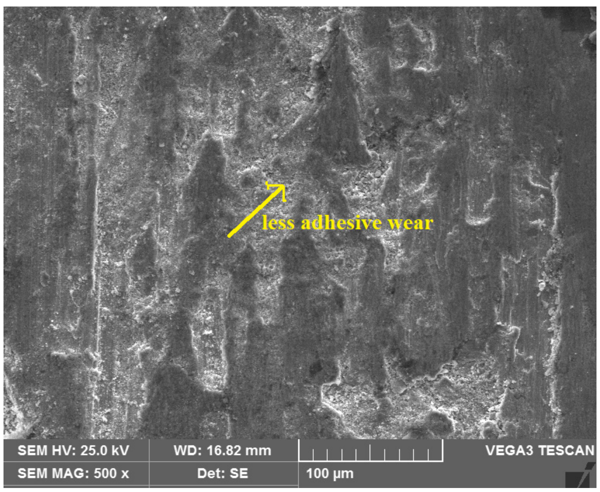

(a)

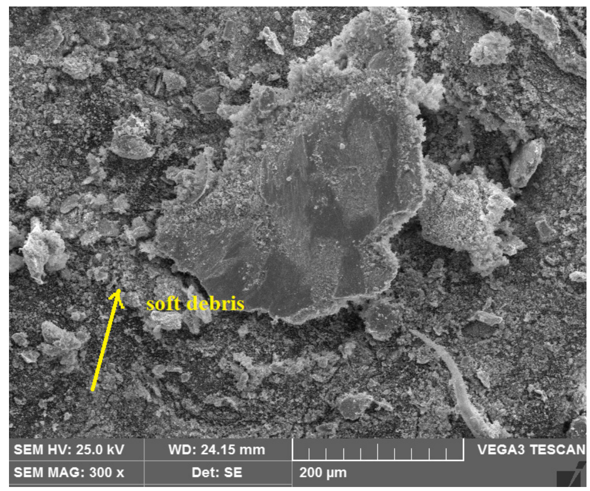

(b)

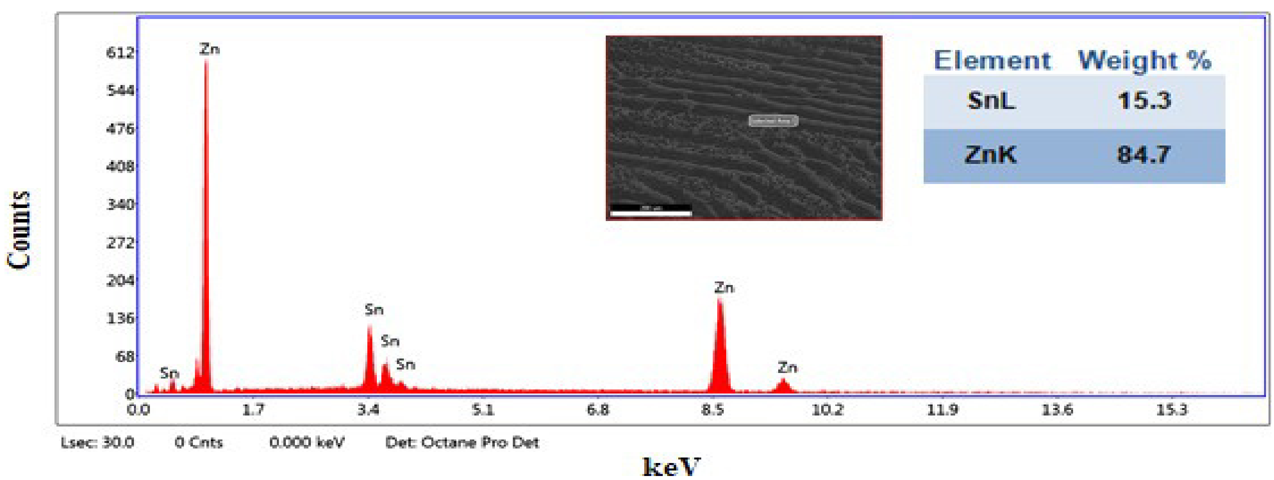

(c)

Figure 5. **(a)**. SEM micrograph of Zn alloy specimen, speed-2.8 m/s, load 40N **(b)** Wear debris micrograph of Zn alloy specimen, speed-2.8 m/s, load 40N with 2000m sliding distance. **(c).** Wear EDS of Zn alloy specimen, speed-1.4 m/s, load 10N.

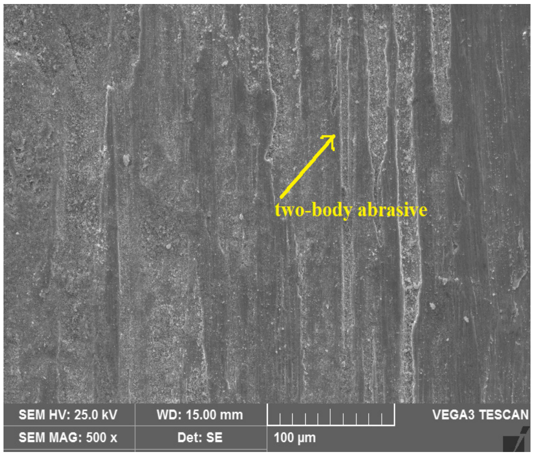

(a)

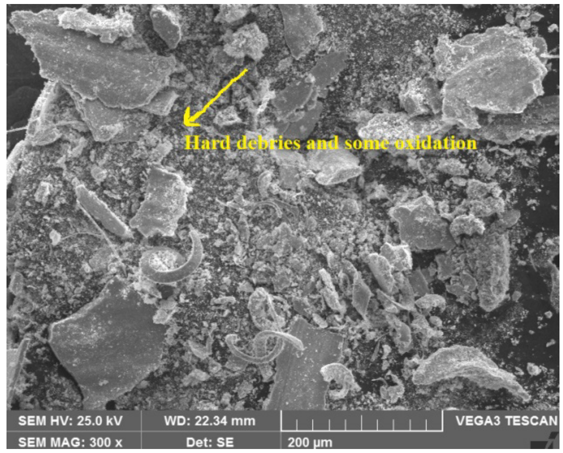

(b)

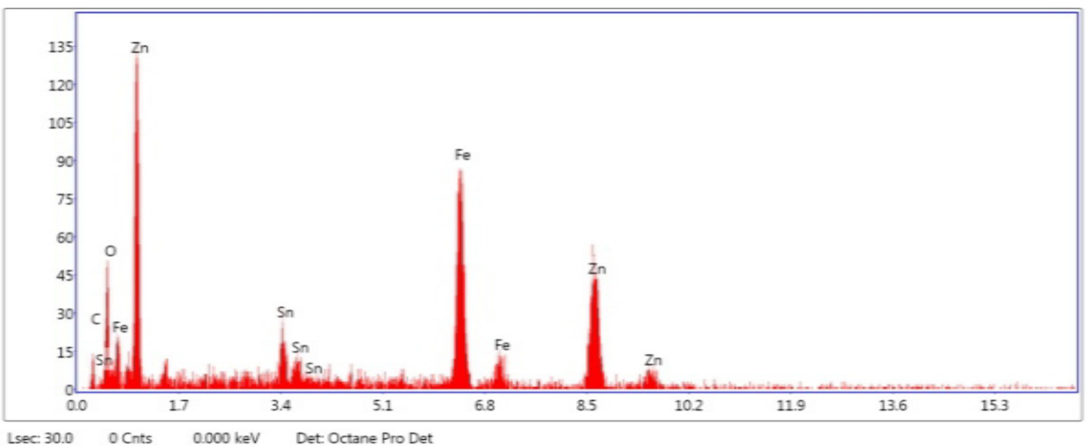

(c)

Figure 6. **(a)** SEM micrograph of 8wt% B_4C specimen, speed-1.4 m/s, load 10N **(b)** Wear debris micrograph of 8wt% B_4C specimen, speed-1.4 m/s, load 10N with 2000m sliding distance. **(c)** Wear EDS of 8wt% wB4C specimen, speed-1.4 m/s, load 10N.

Figure 5(a) depicts the Zn-Sn alloy's wear surface. It demonstrates abrasive, oxidative and delamination types of wear that are operating with greater material loss to indicate severe wear. The soft laminative wear detritus is evident in Figure 5(b). The related EDS verify element presence is seen in Figure 5(c).

Figure 6(a) depicts the Zn-Sn alloy's wear surface at 10N and 1.4m/s. From Figure 6(a), it is evident that the worn surface is composed of an oxide layer and a few minuscule, parallel abrasive grooves that run the length of the surface. This demonstrates that mild abrasive wear is less common and oxidative wear is more common at lower applied pressure[31]. As can be seen in Figure 6(b), wear residues confirm the formation of the oxide layer between both surfaces. At the highest applied pressure of 40N and 2.8m/s, the worn surface for the Zn-Sn alloy with an addition of 8 weight per cent B_4C is depicted in Figure 7(a). It displays highly soft abrasive grooves and is primarily covered in an oxide layer[23]. Corresponding wear debris is seen in Figure 7(b). The worn surface's EDS test reveals that there are oxide layers on all the surfaces depicted in Figure 6(c). This demonstrates that Zn-Sn alloy with an addition of 8 weight per cent B_4C exhibits high wear resistance at 40N higher load.

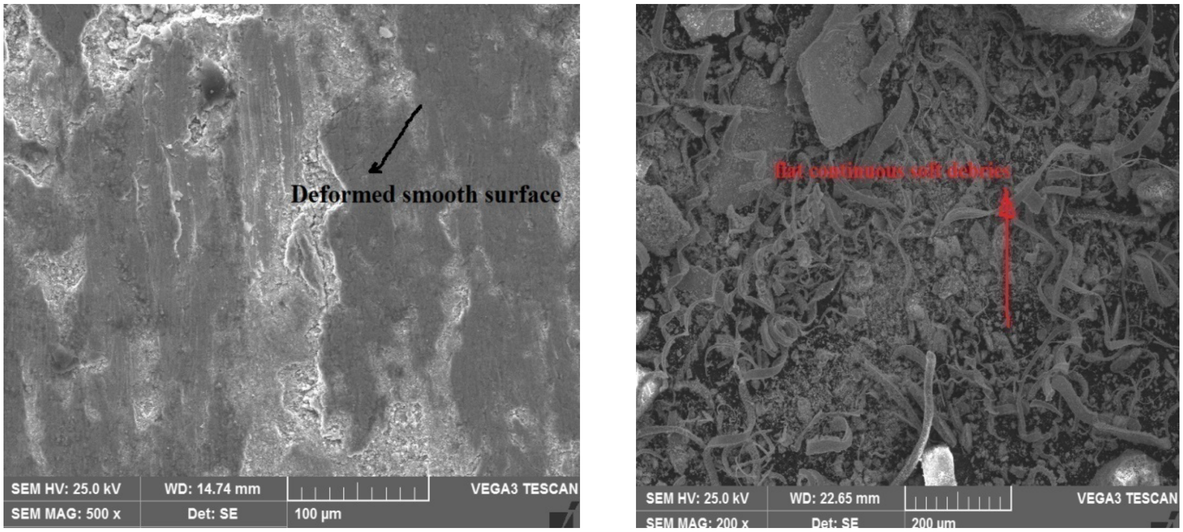

(a) (b)

Figure 7. **(a).** SEM micrograph of 8wt% B_4C specimen, speed-2.8 m/s,. load 40 N **(b)**. Wear debris micrograph of 8wt% wB_4C specimen, speed-2.8 m/s, load 10N with 2000m sliding distance.

4.0 Conclusions

At the tested temperature of 35°C, a higher wear rate % of Zn-Sn alloy is achieved at high pressures, sliding distances and sliding speeds. When compared to cast circumstances under comparable testing settings, the wear rate of Zn alloy with an addition of 8 weight per cent of B_4C is lower. In all of the examples examined, the frictional force showed the same results. The results indicate that the addition of nano B_4C reinforcement improved the mechanical and wear properties of the Zn-Sn alloy, changed the microstructure, and caused an oxide layer to form between both surfaces. Abrasive/oxidative and delaminative wear were the two main wear processes for Zn-Sn alloy, whereas 8 weight per cent of B_4C added to Zn-Sn alloy caused abrasive/oxidative and rich oxide layer formation.

5.0 References

1. Kori SA, Prabhudev MS. Sliding wear characteristics of Al-7Si-0.3mg alloy with minor additions of copper at elevated temperature. Wear. 2011; 271(5-6):680-8. https://doi.org/10.1016/j.wear.2010.12.080
2. BM G, Hindi J, Hegde A, Sharma S, Kini A. Effect of machining parameters on tool life and surface roughness of AISI 1040 dual phase steel, Mater Res. 2022; 25. https://doi.org/10.1590/1980-5373-mr-2021-0351
3. Prajapati JM. Friction and wear behaviour analysis of different journal bearing materials. Mater Sci Eng. 2013; 3(4):2141-6.
4. M. O. F. Technology, Hegde A. Corrosion behaviour of sintered austenitic stainless steel. 2012; 3(12):14-7.
5. Krishnan BR, Ramesh M. Experimental evaluation of Al-Zn-Al2O3 composite on piston analysis by CAE tools. Mech. Mech Eng. 2019; 23(1):212-7. https://doi.org/10.2478/mme-2019-0028
6. Nagesh SN, Siddaraju C, Prakash SV, Ramesh MR. Characterisation of brake pads by variation in composition of friction materials. Procedia Mater Sci. 2014; 5:295-302. https://doi.org/10.1016/j.mspro.2014.07.270
7. Manjunatha S, Manjaiah M, Basavarajappa S. Analysis of factors influencing dry sliding wear behaviour of laser remelted plasma sprayed mo coating using response surface methodology. Arch Metall Mater. 2018; 63(1):217-25. https://doi.org/10.1080/17515831.2017.1407473
8. Anne G, Ramesh MR, Nayaka HS, Arya SB, Sahu S. Microstructure evolution and mechanical and corrosion behaviour of accumulative roll bonded mg-2%Zn/Al-7075 multilayered composite. J Mater Eng Perform.

2017; 26(4):1726-34. https://doi.org/10.1007/s11665-017-2576-z

9. Kumar A, Arafath MY, Gupta P, Kumar D, Hussain CM, Jamwal A. Microstructural and mechano-tribological behaviour of Al reinforced SiC-TiC hybrid metal matrix composite. Mater Today Proc. 2020; 21:1417-20. https://doi.org/10.1016/j.matpr.2019.08.186
10. Liu L, Yang C, Sheng Y. Wear model based on real-time surface roughness and its effect on lubrication regimes. Tribol. 2018; 126:16-20. https://doi.org/10.1016/j.triboint.2018.05.010
11. Kumar GBV, Gowtham P, Sai Ram PNVNS, Sai Ganesh V, Sai Praneeth P. Fabrication and tribological behaviour of Al3003-SiC reinforced MMCs. IOP Conf Ser Mater Sci Eng. 2021; 1185(1):012025. https://doi.org/10.1088/1757-899X/1185/1/012025
12. Ramesh BT. Dry sliding wear test conducted on pin-on-disk testing setup for Al6061-sic metal matrix composites fabricated by powder metallurgy. Int J Innov Sci Eng Technol. 2015; 2(6):264-70.
13. Nagaraj N, Mahendra KV, Nagaral M. Investigations on mechanical behaviour of micro graphite particulates reinforced Al-7Si alloy composites. IOP Conf Ser Mater Sci Eng. 2018, 310(1). https://doi.org/10.1088/1757-899X/310/1/012131
14. Bharath V, Nagaral M, Auradi V, Kori SA. Preparation of 6061Al-Al 2 O 3 MMCs by stir casting and evaluation of mechanical and wear properties. Procedia Mater Sci. 2014; 6:1658-67. https://doi.org/10.1016/j.mspro.2014.07.151
15. Yakoub NG. Effect of nano-zirconia addition on the tribological behaviour of Al-7075 nanocomposites. 2020; 9(8):417-21.
16. Ali A. Wear behaviour of Al6061/TiO2 composites synthesised by stir casting process. J Adv Eng Trends. 2021; 41(2):113-25. https://doi.org/10.21608/jaet.2021.55413.1081
17. Kumar GBV, Panigrahy PP, Nithika S, Pramod R, Rao CSP. Assessment of mechanical and tribological characteristics of silicon nitride reinforced aluminium metal matrix composites. Compos. Part B Eng. 2019; 175:107138. https://doi.org/10.1016/j.compositesb.2019.107138
18. Majzoobi GH, Rahmani K. Mechanical characterisation of Mg-B_4C nanocomposite fabricated at different strain rates. Int J Miner Metall Mater. 2020; 27(2):252-63. https://doi.org/10.1007/s12613-019-1902-x
19. Abbas A, Huang SJ, Ballóková B, Sülleiová K. Tribological effects of carbon nanotubes on magnesium alloy AZ31 and analysing ageing effects on CNTs/AZ31 composites fabricated by stir casting process. Tribol Int 2020; 142. https://doi.org/10.1016/j.triboint.2019.105982
20. Babic M, Ninkovic R, Rato, Rac A. Sliding wear behaviour of zn-al alloys in conditions of boundary lubrication. Ann. Univ. “Dunărea Jos” Galaţi Fascicle 2005; Viii:60-4.
21. Manjunatha TH, Basavaraj Y, Nagaral M, Venkataramana V, Harti JI. Investigations on the mechanical behaviour of Al7075 - nano B_4C composites. IOP Conf Ser Mater Sci Eng. 2018; 376(1):012091. https://doi.org/10.1088/1757-899X/376/1/012091
22. Nagaral M, Auradi V, Prashant SN. Preparation and evaluation of mechanical and wear properties of al6061 reinforced with graphite and Sic. Int J Mech Eng Robot Res. 2012; 1(3):106-12.
23. Rameshkumar T, Rajendran I, Latha AD. Investigation on the mechanical and tribological properties of aluminium-tin based plain bearing material. Tribol Ind. 2010; 32(2):3-10.
24. Nagaral M. Wear behaviour of sic-reinforced Al6061 alloy metal matrix composites by using Taguchi’s techniques. Int J Res Eng Technol. 2014; 3(15):800-4. https://doi.org/10.15623/ijret.2014.0315150
25. Prasad GP, Chittappa HC, Nagaral M, Auradi V. Influence of B_4C reinforcement particles with varying sizes on the tensile failure and fractography of LM29 alloy composites. J Fail Anal Prev. 2020; 20(6):2078-86. https://doi.org/10.1007/s11668-020-01021-6
26. Bharath V, Ajawan SS, Nagaral M, Auradi V, Kori SA. Characterisation and mechanical properties of 2014 aluminium alloy reinforced with Al2O3p composite produced by two-stage stir casting route. J Inst Eng Ser C. 2019; 100(2):277-82. https://doi.org/10.1007/s40032-018-0442-x
27. Baskaran S, Anandakrishnan V, Duraiselvam M. Investigations on dry sliding wear behaviour of in situ casted AA7075-TiC metal matrix composites by using Taguchi technique. Mater Des. 2014; (60):184-92. https://doi.org/10.1016/j.matdes.2014.03.074
28. Adaveesh B, Halesh GM, Nagaral M, Mohan Kumar TS. Microstructure and tensile behaviour of B_4C reinforced ZA43 alloy composites. IOP Conf Ser Mater Sci Eng. 2016; 149(1):012115. https://doi.org/10.1088/1757-899X/149/1/012115
29. Mishra SK, Biswas S, Satapathy A. A study on processing, characterisation and erosion wear behaviour of silicon carbide particle filled ZA-27 metal matrix composites.

Mater Des. 2014; 55:958-65. https://doi.org/10.1016/j.matdes.2013.10.069

30. Manjunatha TH, Basavaraj Y, Venkata Ramana V. Wear analysis of Al7075 alloyed with nano B_4C: A Taguchi approach. Mater Today Proc. 2021; 47(10):2603-7. https://doi.org/10.1016/j.matpr.2021.05.086
31. Harichandran R, Selvakumar N. Microstructure and mechanical characterisation of (B4C+ h-BN)/Al hybrid nanocomposites processed by ultrasound-assisted casting. Int J Mech Sci. 2018; 144:814-26. https://doi.org/10.1016/j.ijmecsci.2017.08.039
32. Wei CB, Tian XB, Yang Y, Yang SQ, Fu RKY, Chu PK. Microstructure and tribological properties of Cu-Zn/TiN multilayers fabricated by dual magnetron sputtering. Surf Coatings Technol. 2007; 202(1):189-93. https://doi.org/10.1016/j.surfcoat.2007.05.013
33. Prabu SB, Karunamoorthy L, Kathiresan S, Mohan B. Influence of stirring speed and stirring time on the distribution of particles in cast metal matrix composite. J Mater Process Technol. 2006; 171(2):268-73. https://doi.org/10.1016/j.jmatprotec.2005.06.071
34. Lo SHJ, Dionne S, Sahoo M, Hawthorne HM. Mechanical and tribological properties of zinc-aluminium metal-matrix composites. J Mater Sci. 1992; 27:8-9. https://doi.org/10.1007/BF01119723
35. Nirmala L, Yuvaraj C, Rao KP. Microstructural and mechanical behaviour of Zinc. IJMET. 2013; 4(4):243-8.
36. Prasad GP, Chittappa HC, Nagaral M, Auradi V. Influence of 40-micron size B_4C particulates addition on the mechanical behaviour of LM29 alloy composites. 2018; 8(2):20-7.
37. Nagaral M, Auradi V, Parashivamurthy KI, Shivananda BK, Kori SA. Dry sliding wear behaviour of aluminium 6061-SiC-graphite particulates reinforced hybrid composites. IOP Conf Ser Mater Sci Eng. 2018; 310(1). https://doi.org/10.1088/1757-899X/310/1/012156
38. Aherwar A, Patnaik A, Pruncu CI. Effect of B_4C and waste porcelain ceramic particulate reinforcements on mechanical and tribological characteristics of high strength AA7075 based hybrid composite. J Mater Res Technol. 2020; 9(5):9882-94. https://doi.org/10.1016/j.jmrt.2020.07.003
39. Narayana K, Naveenn NS. Influence of heat treatment on mechanical and tribological properties of tin brass. Ijmeit. 2014; 2(5):238-43.
40. Singh KM, Chauhan AK. Comparison of mechanical and microstructural examination of Al7075 composites reinforced with micro and nano B_4C. Int J Mech Eng Technol. 2020; 11(4):8-15. https://doi.org/10.34218/IJMET.11.4.2020.002
41. Glaeser WA. Wear properties of heavy-loaded copper-based bearing alloys. Journal of Metals. 1983; 35(10):50-5. https://doi.org/10.1007/BF03338390